IGF binding protein-3 regulates hematopoietic stem cell and endothelial precursor cell function during vascular development

Kyung-Hee Chang*†, Tailoi Chan-Ling‡, Evan L. McFarland‡, Aqeela Afzal†, Hao Pan*†, Louise C. Baxter‡, Lynn C. Shaw*†, Sergio Caballero*†, Nilanjana Sengupta*†, Sergio Li Calzi*†, Sean M. Sullivan§, and Maria B. Grant*†¶

*Program in Stem Cell Biology, †Department of Pharmacology and Therapeutics, and §Department of Pharmaceutics, University of Florida, Gainesville, FL 32610; and ‡Department of Anatomy, University of Sydney, Sydney NSW 2006, Australia

Edited by Judah Folkman, Harvard Medical School, Boston, MA, and approved May 9, 2007 (received for review March 8, 2007)

We asked whether the hypoxia-regulated factor, insulin-like growth factor binding protein-3 (IGFBP3), could modulate stem cell factor receptor (c-kit$^+$), stem cell antigen-1 (sca-1$^+$), hematopoietic stem cell (HSC), or CD34$^+$ endothelial precursor cell (EPC) function. Exposure of CD34$^+$ EPCs to IGFBP3 resulted in rapid differentiation into endothelial cells and dose-dependent increases in cell migration and capillary tube formation. IGFBP3-expressing plasmid was injected into the vitreous of neonatal mice undergoing the oxygen-induced retinopathy (OIR) model. In separate studies, GFP-expressing HSCs were transfected with IGFBP3 plasmid and injected into the vitreous of OIR mice. Administering either IGFBP3 plasmid alone or HSCs transfected with the plasmid resulted in a similar reduction in areas of vasoobliteration, protection of the developing vasculature from hyperoxia-induced regression, and reduction in preretinal neovascularization compared to control plasmid or HSCs transfected with control plasmid. In conclusion, IGFBP3 mediates EPC migration, differentiation, and capillary formation *in vitro*. Targeted expression of IGFBP3 protects the vasculature from damage and promotes proper vascular repair after hyperoxic insult in the OIR model. IGFBP3 expression may represent a physiological adaptation to ischemia and potentially a therapeutic target for treatment of ischemic conditions.

IGFBP3 | angiogenesis | retinopathy of prematurity

Vascular damage associated with diabetic retinopathy and retinopathy of prematurity (ROP) results from tissue ischemia, and, subsequently, this ischemia leads to development of pathological neovascularization. Insulin-like growth factor 1 (IGF1) is required for normal retinal vascular development because vascular development is arrested in its absence despite the presence of VEGF (1). Development of ROP is associated with low levels of IGF1 (2) because the lack of IGF1 in the early neonatal period leads to the development of avascular retina, which results in ROP (3). However, unregulated IGF1 expression can lead to pathological neovascularization (4–13), and IGF1 receptor (IGF1R) antagonists are able to suppress retinal neovascularization *in vivo* by inhibiting VEGF signaling (1).

The effects of IGF1 are mediated by IGF1R and modulated by complex interactions with IGF binding proteins (IGFBPs), which are also modulated at multiple levels. Six IGFBPs function as transporter proteins and storage pools for IGF1 in a tissue- and developmental stage-specific manner. Phosphorylation, proteolysis, polymerization (8), and cell or matrix association (9) regulates the functions of IGFBPs. Specific IGFBPs have been shown to either stimulate or inhibit IGF1 action (10).

IGFBP3, the best studied and most abundant of these binding proteins, carries ≥75% of serum IGF1 and IGF2 in heterotrimeric complexes. Besides its endocrine effects, IGFBP3 has auto- and paracrine actions affecting cell mobility, adhesion, apoptosis, survival, and the cell cycle (14, 15). Like the other IGFBPs, IGFBP3 has IGF1-independent effects. IGFBP3 expression is increased by hypoxic conditions and enhances angiogenesis in some systems while inhibiting it in others (14, 15), thereby demonstrating potentially contradictory effects on the vasculature.

The adult bone marrow (BM)-derived cells participate in normal maintenance and repair of the vasculature in a process called vasculogenesis (16–21). The hypoxia-regulated factors VEGF and stromal-derived factor 1 (SDF1) induce hematopoietic stem cells (HSCs) to leave the BM and enter the circulation; they also induce the HSC progeny, endothelial precursor cells (EPCs), to leave the circulation at sites of ischemic injury to participate in vascular repair (16–19, 22–24). Consequently, we asked whether IGFBP3, which is hypoxia-regulated, could act on HSC/EPC to stimulate migration and vessel formation and influence the participation of these cells in revascularization. For the *in vitro* studies, we used the well characterized human CD34$^+$ EPC population. For *in vivo* studies, we targeted overexpression of IGFBP3 to either the resident retinal vasculature or to HSC and evaluated the vascular response.

Results

IGFBP3 Modulates Migration, Differentiation, and Tube Formation of CD34+ Cells. Fig. 1*A* demonstrates that recombinant human (rh)IGFBP3 stimulates the migration of circulating CD34$^+$ cells in a concentration-dependent manner, whereas circulating CD14$^+$ monocytes, a closely related population of circulating cells, were unresponsive to IGFBP3 (data not shown). IGFBP3 stimulated migration in human retinal endothelial cells, but the response was substantially less than the positive control of 10% FCS (data not shown), whereas the effect of IGFBP3 on CD34$^+$ cells was 6-fold greater than that stimulated by the positive control (10% FCS). Furthermore, CD34$^+$ cells were exquisitely sensitive to IGFBP3, responding dramatically to the lowest concentrations (1 ng/ml) tested. Checkerboard analysis confirmed that the effect was chemotactic and not simply chemokinetic (data not shown). Expression of IGFBP1 and IGF2, also hypoxia-regulated, did not affect CD34$^+$ cell migration (data not shown).

Exposure of CD34$^+$ cells to IGFBP3 reduced expression of CD133 (Fig. 1*B*) and increased endothelial nitric oxide synthase (eNOS) expression (data not shown), thus supporting a role for IGFBP3 in the differentiation of CD34$^+$ cells to endothelial cells.

Increased tissue expression of VEGF and SDF1 occurs in response to ischemic injury. Thus, we asked whether exposure to IGFBP3 would increase expression of VEGF receptors (R1 and

Author contributions: S.M.S. and M.B.G. designed research; K.-H.C., T.C.-L., E.L.M., A.A., H.P., L.C.B., S.C., N.S., S.L.C., and M.B.G. performed research; S.M.S. contributed new reagents/analytic tools; T.C.-L., A.A., L.C.S., and M.B.G. analyzed data; and A.A. and M.B.G. wrote the paper.

The authors declare no conflict of interest.

This article is a PNAS Direct Submission.

Abbreviations: BM, bone marrow; EPC, endothelial precursor cell; *GS* isolectin, *Griffonia simplicifolia* isolectin B4; HSC, hematopoietic stem cell; LDL, low-density lipoprotein; OIR, oxygen-induced retinopathy; P*n*, postnatal day *n*; ROP, retinopathy of prematurity.

¶To whom correspondence should be addressed. E-mail: grantma@pharmacology.ufl.edu.

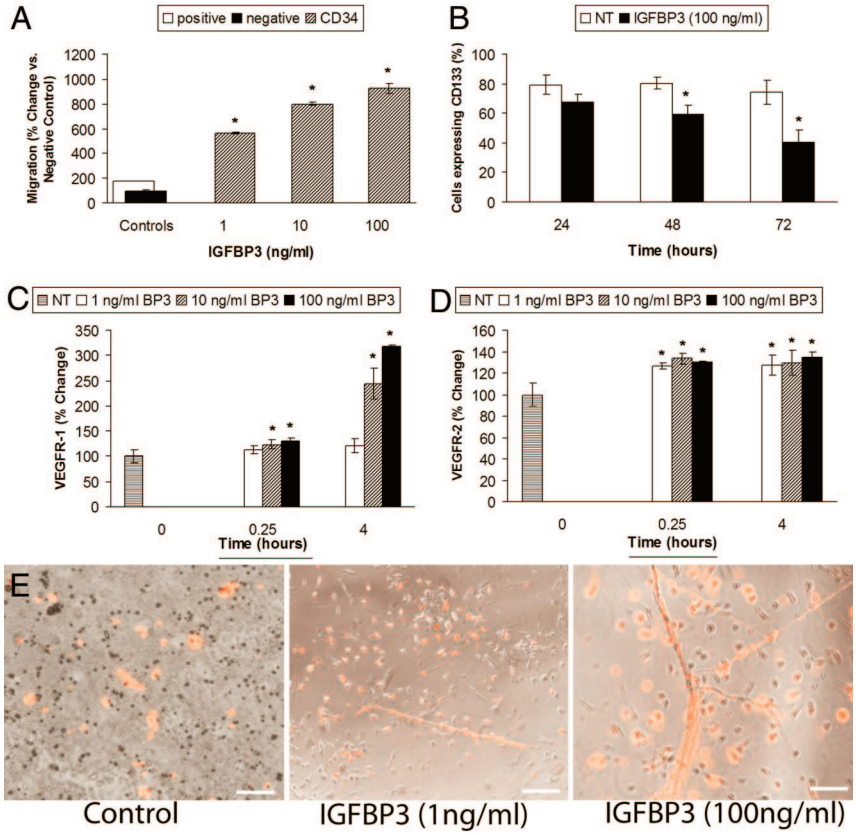

Fig. 1. IGFBP3 modulates CD34$^+$ cell behavior *in vitro*. (*A*) CD34$^+$ cells (hatched bars) migrated in a dose-dependent manner toward IGFBP3. Migration is measured by relative fluorescent units (RFUs) compared to negative control. Negative control, medium alone arbitrarily set at 100 (filled bar); positive control, HPGM medium containing 20% serum (open bar). (*B*) CD34$^+$ cells exposed to IGFBP3 (filled bars) for 48 and 72 h demonstrate reduced CD133 expression, supporting that IGFBP3 promotes their differentiation toward endothelial cells ($P < 0.05$ vs. control shown in open bars). (*C*) IGFBP3 exposure significantly increased VEGFR1 expression in CD34$^+$ cells at the higher concentrations tested. *, $P < 0.05$ vs. control for 15 min and $P < 0.001$ for 4 h. (*D*) IGFBP3 increased the expression of VEGFR2 by 26.58% (*, $P < 0.001$) at 15 min of exposure and by 27.5% ($P < 0.001$) at 4 h of exposure. (*E*) IGFBP3 increases EPC proliferation and tube formation compared to cells treated with control medium. IGFBP3 exposure resulted in a dose-dependent increase in tube formation. The cells have been exposed to fluorescently labeled acetylated LDL. The labeled cells appearing "red" in color represent EPCs that have differentiated into endothelial cells. (Magnification: ×100.) (Scale bars: *Left* and *Center*, 150 μm; *Right*, 100 μm.)

R2) or the SDF1 receptor CXCR4, thus priming CD34$^+$ cells to respond to the growth factor-enriched ischemic retinal environment. Using FACS analysis, VEGFR1, VEGFR2, or CXCR4 levels were examined in CD34$^+$ cells after short exposure to rhIGFBP3. When CD34$^+$ cells were exposed to IGFBP3, there was a dramatic increase in expression of VEGFR1 at 4 h (Fig. 1*C*) and VEGFR2 at 15 min and 4 h (Fig. 1*D*). However, IGFBP3 exposure did not change CXCR4 expression in CD34$^+$ cells (data not shown). The VEGFR1 and VEGFR2 responses to IGFBP3 were selective to CD34$^+$ cells because rhIGFBP3 did not affect the expression of these receptors in CD14$^+$ monocytes, thus supporting the specificity of IGFBP3's effect on EPCs (data not shown).

EPCs that were grown on fibronectin and treated with IGFBP3 showed a dose-dependent qualitative increase in tube formation and acetylated low-density lipoprotein (LDL) incorporation (Fig. 1*E*), further confirming IGFBP3's effect on steps relevant to new blood vessel development.

Expression of IGFBP3 by Proliferating Endothelial Cells Protects from Hyperoxia-Induced Vascular Regression/Obliteration. For the next studies, mouse pups were injected in the vitreous with a plasmid expressing IGFBP3 or with the "empty" cloning vector (control vector) subjected to the oxygen-induced retinopathy (OIR) model and then killed on postnatal day (P)17. The expression of the IGFBP protein was controlled by a proliferating endothelial cell-specific (ET/cdc6) promoter. This promoter has been previously characterized (25, 26). Expression of proteins from this promoter is limited to proliferating endothelial cells of the resident vasculature and has been demonstrated both *in vitro* (26) and *in vivo* (25, 26). This promoter was used to regulate the expression of luciferase in the OIR mouse model, and expression of luciferase was limited to the rapidly proliferating endothelial cells of the retinal vasculature (25).

Fig. 2 shows a quantitative analysis of the vascular density from retinal flat mounts with *Griffonia simplicifolia* isolectin B4 (*GS* isolectin)-stained vessels. Fig. 2 *A–C* shows representative examples of images taken from an eye injected with the IGFBP3-expressing plasmid demonstrating normal appearing vasculature. In contrast, Fig. 2 *D–F* shows images taken from the contralateral uninjected eye from this hyperoxia experimental group, revealing vasoobliterated vessels typical of the OIR model. The vascular remnants in the retinas in uninjected eyes had regions that lacked effective vascular perfusion and had a highly aberrant branching pattern and vascular abnormalities, including reduced capillary density and closure of capillary segments. Fig. 2 *G–I* shows images taken from pups injected with the empty plasmid and exposed to hyperoxia, revealing changes similar to those seen in the contralateral uninjected eye.

IGFBP3 significantly protected the retinal vasculature from hyperoxia-induced vessel regression in midperipheral [$F(2, 42) = 36.40$, $P < 0.001$] and peripheral [$F(2, 42) = 32.33$, $P < 0.001$] regions, but did not have any significant effect on the central region of the retina [$F(2, 42) = 0.37$, $P > 0.05$] (Fig. 2*J*). Injection of IGFBP3-expressing plasmid resulted in the preservation of a vascular bed with a more normal morphology and significantly greater vascular density than eyes in any of the control groups.

Expression of IGFBP3 by Proliferating Endothelial Cells Decreased Preretinal Neovascularization. Neovascularization in the OIR model was evaluated by measuring the reduction in preretinal endothelial nuclei in the IGFBP3-injected pups compared to control pups receiving the empty plasmid (Fig. 3) (25, 27). Expression of IGFBP3 in proliferating resident vasculature resulted in a significant decrease in the number of preretinal nuclei compared to controls. These results are due to protection from hyperoxia-induced vasoobliteration (Fig. 2), which results in less tissue hypoxia during the hypoxic phase of the OIR model.

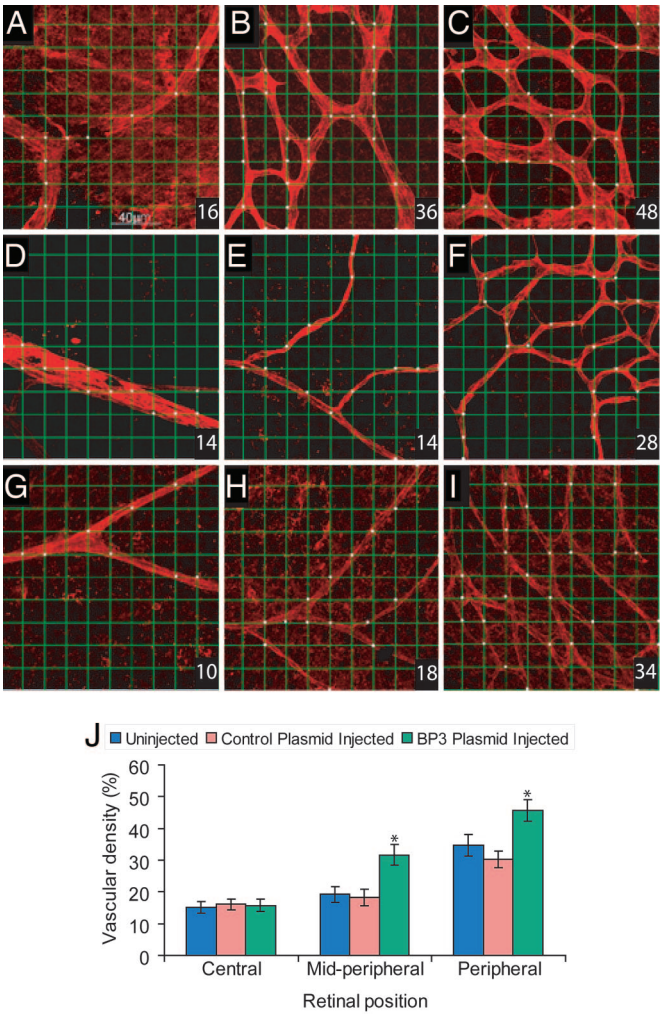

Fig. 2. Quantitative measure of vascular density in the OIR model. Representative fields of view from each of the central, midperipheral, and peripheral retinas captured by using the ×40 objective lens. A 10 × 10 grid was superimposed onto the micrograph, and the incidence of presence of vessels at the intersection points of each grid was determined. The measurement of vascular density was expressed as a percentage from 0 to 100 (bottom right corner of the image). Fields of view selected for analysis included regions of capillary-sized vessels directly adjacent to radial arterioles. (*A–C*) Images taken from eyes injected with IGFBP3 plasmid. Pups were placed in hyperoxia for 5 days and then normoxia for 5 days. (*D–F*) Images taken from contralateral uninjected eyes from the OIR group. (*G–I*) Images taken from empty plasmid-injected eyes from the OIR group. (*J*) One-way ANOVA showed that IGFBP3 protects the retinal vasculature from hyperoxia-induced vessel regression in midperipheral [$F(2, 42) = 36.40$; *, $P < 0.001$] and peripheral [$F(2, 42) = 32.33$; *, $P < 0.001$] regions, but did not have any significant effect on the central region of the retina [$F(2, 42) = 0.37$, $P > 0.05$].

IGFBP3-Expressing HSCs Inhibit Neovascularization by Protecting Neonatal Retinal Vessels from Oxygen-Induced Vasoobliteration. Genetic manipulation of HSCs has been used to both enhance and inhibit neovascularization (28–30). We next used HSCs to deliver IGFBP3 to areas of ischemia and neovascularization. Transfection of HSCs was optimized by using polyethyleneimine (Fig. 4*A*), and expression of IGFBP3 in HSCs was confirmed by real-time RT-PCR (Fig. 4*B*) before injection. To evaluate the effect of the IGFBP3-expressing HSCs on hypoxia-induced vasoproliferation, we examined retinas during the hyperoxic phase of the OIR model (days 7–12) and then during the hypoxic phase on P17 (5 days after return to room air). Using *GS* isolectin conjugated to HRP to provide a low-magnification view of the retinal vasculature, eyes injected with IGFBP3-expressing HSCs showed less pathological neovascularization, almost normal morphology with capillary-free spaces surrounding arterioles, and normal branching patterns (Fig. 4*C*) compared to uninjected eyes or eyes injected with HSCs transfected with the empty vector (Fig. 4*D*).

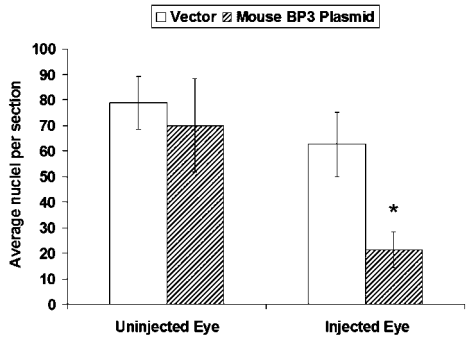

Fig. 3. Intravitreal injection with IGFBP3-expressing plasmid reduces preretinal neovascularization. Neovascularization was evaluated by measuring the reduction in preretinal endothelial nuclei in pups injected with IGFBP3-expressing plasmid (hatched bars) in one eye compared with control pups that received empty plasmid in one eye ($n = 9$, open bars). Uninjected eyes were from the same pups. *, $P < 0.005$ when comparing control plasmid-injected eyes to IGFBP3 plasmid-injected eyes.

GFP$^+$, and therefore HSC-derived, vascular endothelial cells were evident in radial arterioles (Fig. 4 *E* and *F*) in eyes receiving IGFBP3-expressing HSCs.

To further characterize the phenotype of the HSC-derived GFP$^+$ cells, we examined transverse sections of the retinas from these animals to determine whether the GFP$^+$ cells gave rise to vascular endothelial or perivascular cells. Fig. 5 *A* and *B* shows representative cross-sections with GFP$^+$ HSC-derived endothelial cells and pericytes. Fig. 5 *C* and *D* summarizes quantitation of intra- and preretinal vascular density, respectively. In the midperiphery, there was a significant increase in intraretinal and a significant decrease in preretinal vascular density when IGFBP3-expressing HSCs were administered compared to the control conditions of HSCs transfected with control plasmid.

Discussion

IGFBP3 has proangiogenic effects on EPCs promoting the migration, tube formation, and differentiation of these cells into endothelial cells. IGFBP3 expression in the resident vasculature or in HCSs resulted in less vascular regression during hyperoxic injury, increased vessel stabilization, and quicker blood vessel development. These effects led to reduced retinal ischemia when the pups were returned to room air and less neovascularization on P17. Thus, in the same model system, the early enhanced vascular blood vessel formation (proangiogenesis) eliminated ischemia and resulted in reduced preretinal neovascularization later (antiangiogenesis).

In the experiments shown in Figs. 4 and 5, we are using the HSCs to deliver IGFBP3 directly to areas of ischemic injury because these cells specifically home to these sites. HSCs transfected with the plasmid-expressing IGFBP3 increased intraretinal vascular density in the midperiphery while reducing preretinal vascular density in the same region. These studies used a targeted delivery method and corroborated the results obtained with direct intraocular injection of this plasmid.

We also show that specific EPC populations (CD34$^+$ and not CD14$^+$ cells) are modulated by IGFBP3. IGFBP3 acts on multiple steps relevant to promoting differentiation of CD34$^+$ cells into endothelial cells and likely functions to restore perfusion to the ischemic areas by facilitating rapid maturation of the vasculature. This study describes the unique properties of IGFBP3 and focuses

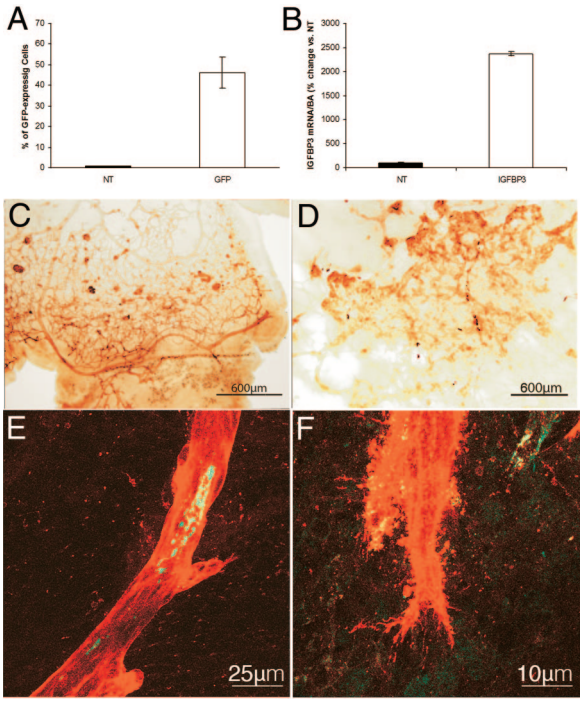

Fig. 4. Retinas from eyes injected intravitreally with HSCs transfected with IGFBP3 and underwent the OIR model. (*A*) HSCs were transfected with 10 μg of DNA of a GFP plasmid (open bars) by using either Lipofectamine transfection reagent or polyethyleneimine. Mock-transfected cells did not contain any DNA (filled bars). GFP expression in the cells was assessed by flow-cytometry analysis. Cells that underwent mock transfection did not show GFP cells, whereas polyethyleneimine showed increased transfection compared to Lipofectamine. (*B*) Transfection of GFP HSC with IGFBP3-expressing plasmid (open bars) results in a 25-fold increase in IGFBP3 expression *in vitro* compared with nontransfected (NT) controls (filled bars). (*C* and *D*) Low-magnification views of *GS* isolectin-labeled vasculature in the retina from a pup injected with IGFBP3-transfected HSCs (*C*) compared with the contralateral uninjected eye (*D*). (*C*, *E*, and *F*) HSC-IGFBP3 animal showed a vascular tree with more normal morphology, with a mature pattern of differentiation, normal dichotomous branching pattern, and less abnormal vascularization. (*E* and *F*) Retinal flat mounts demonstrate the localization of GFP HSCs within the vasculature. Merged green (HSC) and red (resident vasculature) channels demonstrating the localization of HSCs within the *GS* isolectin-labeled vasculature (red). There is evidence of GFP HSC incorporation (yellow) in vascular endothelial cells lining neovascular lumens (*E*) and filopodia spread from neovascular clumps (*F*).

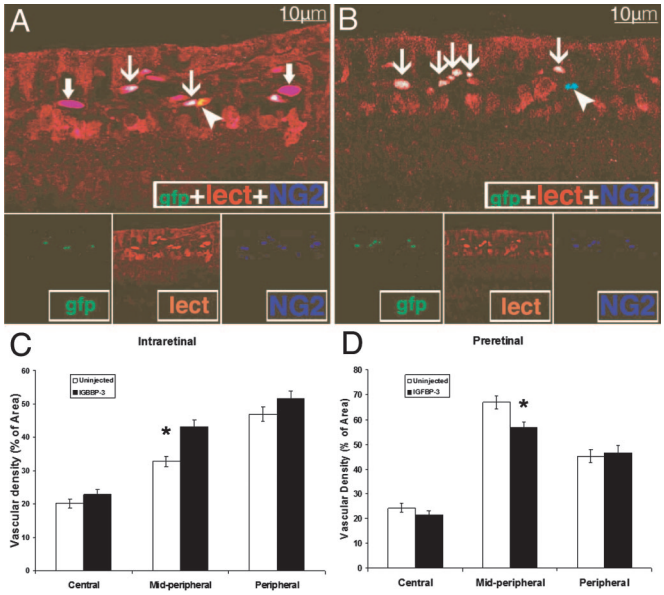

Fig. 5. IGFBP3-expressing HSCs give rise to vascular endothelial and perivascular cells, and injection of IGFBP3 HSCs during the hypoxic phase of the OIR model results in decreased preretinal neovascularization. (*A* and *B*) Cryostat sections from IGFBP3-injected eyes showing GFP HSC-derived cells giving rise to vascular endothelial as well as perivascular cells. Isolectin stains endothelial and perivascular cells, whereas NG2 is a pericyte marker. Thin arrows in *A* and *B* mark triple-labeled (NG2$^+$/GFP$^+$/isolectin$^+$) cells representing vasculature where GFP HSCs have become endothelial cells or pericytes. Thick arrows (*A*) show two NG2$^+$/isolectin$^-$/GFP$^+$ HSC-derived pericytes within regions of the resident vasculature. Arrowhead in *A* shows an NG2$^-$/isolectin$^+$/GFP$^+$ HSC-derived endothelial cell (yellow). Arrowhead in *B* shows an NG2$^+$/isolectin$^-$/GFP$^+$ resident pericyte (pale blue). (*C* and *D*) Vascular density measured from the intraretinal vessels (*C*) or from the preretinal vessels (*D*). (*C*) Vascular density measurements (intraretinal vessels) showed a significant difference in the vessels in the midperipheral region between eyes injected with HSC transfected with control plasmid vs. HSCs transfected with IGFPB3 plasmid (*, $P < 0.003$). (*D*) Vascular density measurements (preretinal vessels) showed a significant difference in the vessels in the midperipheral region between eyes injected with HSC transfected with control plasmid vs. HSCs transfected with IGFBP3 plasmid (*, $P < 0.0008$).

attention on this protein as a factor that regulates HSC and EPC behavior by facilitating their participation in vascular repair and development. We postulate that, under conditions of hypoxia, IGFBP3 expressed by ischemic tissue could stimulate HSC migration, promoting recruitment from the circulation into areas of ischemic injury. Furthermore, IGFBP3 facilitates migration and tube formation of these cells, which are steps required for new blood vessel formation and repair at sites of injury, ultimately restoring blood flow and relieving ischemia. By promoting rapid differentiation of a "beneficial" EPC population (i.e., CD34$^+$ cells, rather than the deleterious CD14$^+$ cell population), IGFBP3 facilitates proper vascular repair (CD34$^+$ cell-mediated) and minimizes the inflammatory component of vascular repair (CD14$^+$ cell-mediated) (31, 32).

Urbich *et al.* (33) found that IGF1 mRNA was highly expressed in CD34$^+$ cells relative to mature endothelial cells or CD14$^+$ monocytes, which produce ≈10-fold less IGF mRNA. IGF1 is needed for survival of EPC populations in culture, and thus modulation by IGFBPs, including IGFBP3, is certainly plausible (34). Previously, we showed that quiescent human retinal endothelial cells (representing the resident endothelial cells of the retina) express high levels of IGFBP3 (35). In contrast, CD34$^+$ cells have undetectable levels, making these immature cells very sensitive to small increases in endogenous tissue levels of IGFBP3 or exogenous administration of IGFBP3 as observed in the migration assays.

The profound stimulatory effects of IGFBP3 on HSC/EPC occur at low concentrations, are cell type-specific (CD34$^+$ cells and not CD14$^+$ cells), and are context-dependent (protective during hyperoxic injury). The concentration of IGFBP3 used here represents one of the lowest ever shown to have an *in vitro* effect (15, 36–40).

Our work supports that of Liu *et al.* (41), who showed, by using *in vitro* cell proliferation assays, that the addition of exogenous IGFBP3 to cultures of purified CD34$^+$ CD38-Lin$^-$ cells stimulated the proliferation of these primitive hematopoietic cells, suggesting that IGFBP3 is capable of expanding primitive human blood cells.

In complementary work in this issue of PNAS, Lofqvist *et al.* (42) show a dose-dependent increase in vessel survival and retinal vessel regrowth with increasing IGFBP3. In infants, lower IGF1 and IGFBP3 correlated with more severe ROP. They conclude, as we have, that IGFBP3 helps to prevent oxygen-induced vessel loss and promote vascular regrowth after vascular destruction *in vivo*, and that an increase in vessel survival prevents hypoxia-induced neovascularization and ROP. They also find that the IGFBP3 effect is independent of IGF1.

In conclusion, we describe IGFBP3 as a factor that modulates vascular precursor function and provides a possible mechanism for the varied and contradictory effects previously observed with IGFBP3. IGFBP3 has been described as both pro- and antiangiogenic. Our studies demonstrate that IGFBP3 has direct proangiogenic effects on $CD34^+$ cell migration, differentiation, and tube formation, steps required for proper vascular repair after hypoxic injury. IGFBP3 also has vascular stabilizing effects as shown by its ability to prevent oxygen-induced vasoobliteration and regression and ultimately reduced pathological preretinal neovascularization in the OIR model. Thus, we postulated that hypoxia-induced increases in IGFBP3 expression may represent part of the retina's (and perhaps other tissues') physiological response to hypoxia and may facilitate proper revascularization and repair after ischemic injury. Exogenous administration of IGFBP3 may represent an approach to treatment of conditions associated with pathological neovascularization as well as inadequate vascular repair.

Materials and Methods

Preparation of $CD34^+$ and $CD14^+$ Cells. Mobilized human $CD34^+$ and $CD14^+$ cells were purchased commercially (Cambrex Bio Science Walkersville, Walkersville, MD) and maintained in an undifferentiated state per the manufacturer's protocol.

Flow-Cytometry Analysis. Changes in the expression of VEGF receptor, eNOS protein, and CD133 surface antigen in $CD34^+$ cells were evaluated after with IGFBP3. Expression levels for the VEGF receptors and CXCR-4 on $CD34^+$ cells were examined after incubation (5% CO_2 and 37°C) with 100 ng/ml IGFBP3 (0 min, 15 min, or 4 h). After treatment, the cells were permeabilized by using a Cytofix/Cytoperm kit (BD Bioscience, San Diego, CA). The cells were then blocked with 10% normal human serum (Jackson ImmunoResearch Laboratories, West Grove, PA). Next, 10 μg of anti-Flt-1 (VEGFR1) (Santa Cruz Biotechnology, Santa Cruz, CA), 10 μg of anti-VEGFR2 antibody (NeoMarkers, Fremont, CA), or 20 μg of anti-CXCR4 antibody (BD Biosciences) was added to cells, and cells were then incubated on ice for 30 min. Cells were washed with PBS and incubated with 23 μg of FITC-conjugated goat anti-mouse (Jackson ImmunoResearch Laboratories) on ice for 30 min. The cells were washed in PBS and analyzed by flow cytometry. Anti-GFP (Molecular Probes, Carlsbad, CA) was used as an isotype control.

Expression of CD133 was evaluated by using a phycoerythrin-labeled antibody (Miltenyi Biotec, Auburn, CA). $CD34^+$ cells were incubated with or without IGFBP3 for $\leq$72 h at 5% CO_2 at 37°C. Phycoerythrin-conjugated mouse IgG_a, κ-Ig isotype control monoclonal antibody (BD Bioscience) was used as an isotype control. Apoptotic dead cells were removed before analysis by 7-aminoactinomycin D (Sigma–Aldrich, St. Louis, MO) positive selection.

Data were acquired with a FACSCalibur flow cytometer (BD Biosciences) and analyzed with BD CellQuest (BD Biosciences).

EPC Tube Formation. Peripheral blood from healthy volunteers giving informed consent under a protocol approved by the Institutional Review Board was collected in cell preparation tubes with heparin (BD Biosciences). Mononuclear cells were isolated by centrifugation in a swinging bucket rotor at 1,800 $\times$ *g* for 20 min at room temperature. The cells were cultured on fibronectin-coated dishes with Endocult Stem Cell liquid media (Stem Cell Technologies, Vancouver, BC, Canada) per the manufacturer's protocol. IGFBP3 was added to the cultures at 0, 1, 10, and 100 ng/ml, and the cells were examined microscopically 5 days later. After *in vitro* exposure to recombinant human IGFBP3 (Upstate Cell Signaling Solutions, Lake Placid, NY), the endothelial nature of the cells was confirmed with incorporation of 1,1′-dioctadecyl-3,3,3′3′-tetramethylindocarbocyanine perchlorate-labeled acetylated-LDL (Molecular Probes) with 50 μg/ml final concentration. Digital image captures were made with a Zeiss Axiovert 135 (Carl Zeiss, Thornwood, NY) coupled to a Hamamatsu CCD camera (Hamamatsu Corporation, Bridgewater, NJ).

Quantitative Real-Time RT-PCR. Total mRNA of HSCs was isolated by using the Total RNA Mini Kit (Bio-Rad, Hercules, CA). The mRNA was transcribed by using an iScript cDNA Synthesis Kit (BioRad), and real-time PCR was performed by using an iQ SYBR Green Supermix (Bio-Rad). Primers for the PCR were mouse IGFBP3 forward (5′-CCA ACC TGC TCC AGG AAA CA-3′) and reverse (5′-GTG GCC TTT TTT GAT GAC ATC C-3′). All samples were normalized to β-actin (Ambion, Austin, TX). Real-time PCR was performed on a DNA engine Opticon system (MJ Research, Waltham, MA) for 60 cycles. All reactions were performed in triplicate.

Chemotaxis Assay. $CD34^+$ and $CD14^+$ cell migration was performed as previously described (43). Briefly, $CD34^+$ or $CD14^+$ cells were stained with Calcein-AM (Molecular Probes) before loading them onto the Boyden Chamber. PBS containing 1 to 100 ng/ml IGFBP3 (Upstate, Charlottesville, VA) was loaded in the bottom chamber, which was overlaid with a polycarbonate membrane (8-μm pores) (Neuro Probe, Gaithersburg, MD) coated with 10% bovine collagen, and then the cells were loaded in the top chamber. After 4.5 h at 5% CO_2 at 37°C, the percentage of cells that migrated was determined by collecting the media in the lower chamber and determining the relative fluorescence measured as relative fluorescence units by using a Synergy HT (Bio-Tek Instruments, Winooski, VT) with an excitation of 485 $\pm$ 20 nm and an emission of 528 $\pm$ 20 nm.

Human retinal endothelial cells were isolated and cultured (44), and migration in response to IGFBP3 was performed as previously described (45). Briefly, when the human retinal endothelial cells reached 70% confluence, the cells were dissociated by using trypsin–EDTA (catalog no. T4299; Sigma–Aldrich). The cells were washed and resuspended in DMEM to a concentration of 1,000 cells per μl, and 30 μl of cells were then added to each well of a blind well chemotaxis chamber. The wells were overlaid with a porous polyvinylpyrrolidone-free polycarbonate membrane (12-μm pores) that had been coated with 10% bovine collagen. The chemotaxis chamber was inverted and incubated at 37°C for 4 h in a humidified incubator. The chambers were then placed upright, and 50 μl of a solution containing various concentrations of IGFBP3 (1, 10, and 100 ng/ml) were added to the upper wells. DMEM was used as a negative control to evaluate random cell migration, whereas 10% FBS served as a positive control. The chambers were incubated for an additional 12 h. The membranes were collected, and cells on the attachment (lower) side were scraped, leaving behind cells that migrated through the pores of the membrane. The membranes were fixed, stained with Leukostat Solution (Fisher, Springfield, NJ), and attached to glass slides. The cells were counted under a light microscope, and the number of migrating cells per well was calculated by averaging the number of cells counted in three separate high-power fields. The counts for three replicate wells were averaged.

GFP HSC Transfection with Plasmid-Expressing IGFBP3. Highly enriched sca-1^+, c-kit^+, Lin^- HSCs were obtained from homozygous transgenic GFP mouse donors as previously described (46). Cells were transfected with the plasmid-overexpressing IGFBP3 driven by a proliferating endothelial cell-specific promoter composed of 7 $\times$ 46-mer multimerized endothelin enhancer upstream of a human Cdc6 promoter (25, 26) by using polyethylenimine/plasmid complexes (47). Transfection efficiency of 40% was typically observed.

Experimental Animals. All animal procedures used were in agreement with the National Institutes of Health Guide for the Care and Use of Laboratory Animals and were approved by the University

of Florida Institutional Animal Care and Use Committee. Timed-pregnant C57BL/6J mice were purchased from The Jackson Laboratory (Bar Harbor, ME).

OIR Model and Enhanced IGFBP3 Expression. Mice were injected with either a plasmid-expressing mouse IGFBP3 under control of the proliferating endothelial cell-specific promoter (25) or "empty" cloning vector on P1 in a volume of 0.5 μl per eye. By using a proliferating endothelial cell-specific promoter, IGFBP3 expression was targeted to areas of neovascularization as previously described (25, 26). On P7, the pups were placed into high oxygen (75%) for 5 days, returned to room air, and then killed at P17. Eyes from mice injected with the plasmid-expressing IGFBP3 ($n = 9$) were compared to eyes from mice injected with empty cloning vector ($n = 9$) or the uninjected eye of the same animal.

A second cohort of mice ($n = 18$) was injected on P1 with GFP^+ mouse HSC (5×10^3 cells per eye in 0.5-μl injection volume) transfected with the identical plasmid as described above. The mice were subjected to 5 days of hyperoxia from P7 to P12 and killed at P17. Data from these mice were compared to the uninjected eye of the same animal or with mice injected with GFP^+ mouse HSC transfected with empty cloning vector ($n = 18$).

***GS* Isolectin and GFP Double-Label Immunohistochemistry.** Retinal whole mounts were prepared as described previously (48). *GS* isolectin (Sigma–Aldrich) and two antibodies against GFP (chicken anti-GFP or mouse anti-GFP/EGFP, both from Chemicon, Temecula, CA) were used to covisualize GFP cells with the vasculature.

***GS* Isolectin Conjugated to HRP.** Retinal whole mounts ($n = 6$) were processed as described previously (48) and then incubated in *GS* isolectin peroxidase conjugate (Sigma–Aldrich) for 4 h. The retinas were processed as reported previously (49, 50).

Microscopy and Mapping. Retinal whole mounts ($n = 6$) were examined by both deconvolution and confocal microscopy. For deconvolution fluorescence microscopy and photography, we used a Zeiss microscope (model Axioplan 2 attachment HBO 100; Carl Zeiss) and Axiocam HRm camera (Thornwood, NY). Confocal microscopy was performed with a Leica argon–krypton laser mounted on a Leica DMRBE epifluorescence photomicroscope (Leica, Wetzlar, Germany). Alexa Fluor 488 and Cy3 fluorescence was excited sequentially at 488 and 550 nm, respectively. Images were processed with Adobe Photoshop 5.0 software (Adobe Systems, Mountain View, CA).

Vascular Density Analysis. To obtain a quantitative measure of vascular density for each experimental condition, we developed a measure of vascular density expressed as a percentage from 0 to 100. After *GS* isolectin histochemistry, representative fields of views from each of the central, midperipheral, and peripheral retinas were captured by using the $\times 40$ objective lens. Fields of view selected for analysis in peripheral retinas included regions of capillary-sized vessels directly adjacent to radial arterioles, whereas areas selected for analysis in central and midperipheral retinas included the radial arteriole. A 10×10 grid was superimposed onto the micrograph as previously described (51), and the incidence of presence or absence of vessels at the intersection points of each grid was determined. The mean vascular density incidence was determined for each area and compared to its control. The data are presented as means $\pm$ SD. The statistical significance of differences among mean values was determined by one-way ANOVA and the Tukey HSD multiple comparison post hoc test for the hyperoxia experiments, and a two-tailed t test was used for the hypoxic experiment. ANOVA statistical analysis was performed with SPSS 13.0 software (SPSS, Chicago, IL), and two-tailed t test statistical analysis was performed with a P value of <0.05.

We thank Myphoung Le for her efforts in cloning the mouse IGFBP3. This work was supported by National Institutes of Health Grants EY007739 and EY012601 (to M.B.G.), the Juvenile Diabetes Research Foundation, International Science Linkages Grant CG100045 (to T.C.-L.), and National Health and Medical Research Council of Australia Grants 402824 and 464859 (to T.C.-L.).

1. Smith LE, Shen W, Perruzzi C, Soker S, Kinose F, Xu X, Robinson G, Driver S, Bischoff J, Zhang B, *et al*. (1999) *Nat Med* 5:1390–1395.
2. Hellstrom A, Engstrom E, Hard AL, Albertsson-Wikland K, Carlsson B, Niklasson A, Lofqvist C, Svensson E, Holm S, Ewald U, *et al*. (2003) *Pediatrics* 112:1016–1020.
3. Lofqvist C, Engstrom E, Sigurdsson J, Hard AL, Niklasson A, Ewald U, Holmstrom G, Smith LE, Hellstrom A (2006) *Pediatrics* 117:1930–1938.
4. Grant MB, Russell B, Fitzgerald C, Merimee TJ (1986) *Diabetes* 35:416–420.
5. Grant MB, Wargovich TJ, Ellis EA, Tarnuzzer R, Caballero S, Estes K, Rossing M, Spoerri PE, Pepine C (1996) *Regul Pept* 67:137–144.
6. Grant MB, Caballero S, Bush DM, Spoerri PE (1998) *Diabetes* 47:1335–1340.
7. Grant MB, Caballero S, Tarnuzzer RW, Bass KE, Ljubimov AV, Spoerri PE, Galardy RE (1998) *Diabetes* 47:1311–1317.
8. Sakai K, Busby WH, Jr, Clarke JB, Clemmons DR (2001) *J Biol Chem* 276:8740–8745.
9. Moralez A, Busby WH, Jr, Clemmons D (2003) *Endocrinology* 144:2489–2495.
10. Firth SM, Baxter RC (2002) *Endocr Rev* 23:824–854.
11. Poulsen JE (1953) *Diabetes* 2:7–12.
12. Merimee TJ, Zapf J, Froesch ER (1983) *N Engl J Med* 309:527–530.
13. Grant MB, Schmetz I, Russell B, Harwood H, Jr, Silverstein J, Merimee TJ (1986) *J Clin Endocrinol Metab* 63:981–984.
14. Granata R, Trovato L, Garbarino G, Taliano M, Ponti R, Sala G, Ghidoni R, Ghigo E (2004) *Faseb J* 18:1456–1458.
15. Liu B, Lee KW, Li H, Ma L, Lin GL, Chandraratna RA, Cohen P (2005) *Clin Cancer Res* 11:4851–4856.
16. Crosby JR, Kaminski WE, Schatteman G, Martin PJ, Raines EW, Seifert RA, Bowen-Pope DF (2000) *Circ Res* 87:728–730.
17. Kocher AA, Schuster MD, Szabolcs MJ, Takuma S, Burkhoff D, Wang J, Homma S, Edwards NM, Itescu S (2001) *Nat Med* 7:430–436.
18. Lagaaij EL, Cramer-Knijnenburg GF, van Kemenade FJ, van Es LA, Bruijn JA, van Krieken JH (2001) *Lancet* 357:33–37.
19. Quaini F, Urbanek K, Beltrami AP, Finato N, Beltrami CA, Nadal-Ginard B, Kajstura J, Leri A, Anversa P (2002) *N Engl J Med* 346:5–15.
20. Hill JM, Zalos G, Halcox JP, Schenke WH, Waclawiw MA, Quyyumi AA, Finkel T (2003) *N Engl J Med* 348:593–600.
21. Schmidt-Lucke C, Rossig L, Fichtlscherer S, Vasa M, Britten M, Kamper U, Dimmeler S, Zeiher AM (2005) *Circulation* 111:2981–2987.
22. Adamis AP, Shima DT (2005) *Retina* 25:111–118.
23. Butler JM, Guthrie SM, Koc M, Afzal A, Caballero S, Brooks HL, Mames RN, Segal MS, Grant MB, Scott EW (2005) *J Clin Invest* 115:86–93.
24. Sengupta N, Caballero S, Mames RN, Timmers AM, Saban D, Grant MB (2005) *Invest Ophthalmol Vis Sci* 46:343–348.
25. Shaw LC, Pan H, Afzal A, Calzi SL, Spoerri PE, Sullivan SM, Grant MB (2006) *Gene Ther* 13:752–760.
26. Szymanski P, Anwer K, Sullivan SM (2006) *J Gene Med* 8:514–523.
27. Shaw LC, Afzal A, Lewin AS, Timmers AM, Spoerri PE, Grant MB (2003) *Invest Ophthalmol Vis Sci* 44:4105–4113.
28. Becker CM, Farnebo FA, Iordanescu I, Behonick DJ, Shih MC, Dunning P, Christofferson R, Mulligan RC, Taylor GA, Kuo CJ, Zetter BR (2002) *Cancer Biol Ther* 1:548–553.
29. Karlsson S, Ooka A, Woods NB (2002) *Haemophilia* 8:255–260.
30. Logan AC, Lutzko C, Kohn DB (2002) *Curr Opin Biotechnol* 13:429–436.
31. Anghelina M, Krishnan P, Moldovan L, Moldovan NI (2006) *Am J Pathol* 168:529–541.
32. Anghelina M, Moldovan L, Zabuawala T, Ostrowski MC, Moldovan NI (2006) *J Cell Mol Med* 10:708–715.
33. Urbich C, Dimmeler S (2004) *Circ Res* 95:343–353.
34. Kim JJ, Buzzio OL, Li S, Lu Z (2005) *Biol Reprod* 73:833–839.
35. Spoerri PE, Caballero S, Wilson SH, Shaw LC, Grant MB (2003) *Invest Ophthalmol Vis Sci* 44:365–369.
36. Rajah R, Valentinis B, Cohen P (1997) *J Biol Chem* 272:12181–12188.
37. Franklin SL, Ferry RJ, Jr, Cohen P (2003) *J Clin Endocrinol Metab* 88:900–907.
38. Lee KW, Ma L, Yan X, Liu B, Zhang XK, Cohen P (2005) *J Biol Chem* 280:16942–16948.
39. Benini S, Zuntini M, Manara MC, Cohen P, Nicoletti G, Nanni P, Oh Y, Picci P, Scotlandi K (2006) *Int J Cancer* 119:1039–1046.
40. Jerome L, Alami N, Belanger S, Page V, Yu Q, Paterson J, Shiry L, Pegram M, Leyland-Jones B (2006) *Cancer Res* 66:7245–7252.
41. Liu LQ, Sposato M, Liu HY, Vaudrain T, Shi MJ, Rider K, Stevens Z, Visser J, Deng HK, Kraus M (2003) *Oncol Res* 13:359–371.
42. Lofqvist C, Chen J, Connor K, Smith A, Aderman CM, Liu N, Pintar J, Ludwig T, Hellstrom A, Smith L (2007) *Proc Natl Acad Sci USA* 104:10589–10594.
43. Segal MS, Shah R, Afzal A, Perrault CM, Chang K, Schuler A, Beem E, Shaw LC, Li Calzi S, Harrison JK, *et al*. (2006) *Diabetes* 55:102–109.
44. Grant MB, Guay C (1991) *Invest Ophthalmol Vis Sci* 32:53–64.
45. Grant MB, Jerdan J, Merimee TJ (1987) *J Clin Endocrinol Metab* 65:370–371.
46. Grant MB, May WS, Caballero S, Brown GA, Guthrie SM, Mames RN, Byrne BJ, Vaught T, Spoerri PE, Peck AB, Scott EW (2002) *Nat Med* 8:607–612.
47. Shin JY, Suh D, Kim JM, Choi HG, Kim JA, Ko JJ, Lee YB, Kim JS, Oh YK (2005) *Biochim Biophys Acta* 1725:377–384.
48. Chan-Ling T (1997) *Microsc Res Tech* 36:1–16.
49. Chan-Ling TL, Halasz P, Stone J (1990) *Curr Eye Res* 9:459–478.
50. Medana IM, Hunt NH, Chan-Ling T (1997) *Glia* 19:91–103.
51. Chen-Ling T, Page M, Gardiner T, Baxter L, Hughes S (2004) *Am J Pathol* 165:1301–1313.